Available online at www.sciencedirect.com

ScienceDirect

Procedia Technology 10 (2013) 53 – 61

Procedia Technology

International Conference on Computational Intelligence: Modeling Techniques and Applications (CIMTA) 2013

Hybrid computational simulation and modeling assisted structural analysis of anti-tubercular molecules

Sudipta Mondal[a], Neeraj Upamanyu[b], Debanjan Sen[a]*

[a]*Bengal Institute of Pharmaceutical Sciences, Kalyani, Nadia,West Bengal, 741235,India*
[b]*RKDF College of Pharmacy, Bhopal, MP,India*

Abstract

Tuberculosis (TB), a leading cause of death worldwide, in association with HIV-AIDS and the emergence of multi-drug resistance (MDR) or extensively drug resistance (XDR) strains, has created necessity to develop new class of anti-tubercular drug. Strategic implementation of hybrid computational simulation and searching method has been used to analyze and explore new chemical entity effective against MDR Tuberculosis strains. Initially a ligand-based pharmacophore hypothesis and 3D Quantitative structure activity relationship (QSAR) model with statistical significance (R^2=0.985, SD=0.146, Pearson R=0.936, Q2= 0.849, R^2_{Pred}=0.851, $Q^2_{(F2)}$=0.854) was generated by well validated algorithm. Concurrently molecular docking analysis was performed by considering three individual grid points of InhA enzyme. Moreover Ligand-based pharmacophoric model was drastically re-assessed against receptor-based docking simulation model to authenticate this *in silico* trialing. The docking analysis indicates that this class of ligands nicely occupies the hydrophobic pocket of InhA enzyme, which is an important feature of *direct* InhA inhibitors and it reveals that the chemical entities can inhibit the aforementioned enzyme without activating katG (a catalase/peroxidase enzyme) enzyme pathway.

Selection and peer-review under responsibility of the University of Kalyani, Department of Computer Science & Engineering

Keywords: Tuberculosis; Molecular modeling; QSAR; Docking; InhA; MDR-TB; Cinnamic acid

1. Introduction

Mycobacterium tuberculosis, a single infectious agent causing Tuberculosis(TB) that kills more than three million

* Corresponding author. Tel.: +91-9046818566; fax: +33-2589-1742.
E-mail address: debanjan.sen@bipstrust.org

Selection and peer-review under responsibility of the University of Kalyani, Department of Computer Science & Engineering
doi:10.1016/j.protcy.2013.12.336

people worldwide every year and every third individual of world has been exposed to or infected to *M. tuberculosis* [1,2,3]. The global incidence rate of TB is growing at 1.1% per year and the number of cases at 2.4% per year [1].The high susceptibility of HIV-AIDS infected people to this disease and co-infection of two pathogens is accelerating the collapse of immune system [2, 4]. About 3.7 million of new TB patient have multi drug resistant strains (MDR-TB), defined as resistant to at least Isoniazid (INH) and Rifampicin [5]. WHO has estimated that there are about 0.5 million cases of MDR TB and among this about 9% is extensively drug resistant strains(XDR TB), strains that are resistant to Isoniazid and Rifampicin , as well as any fluoro-quinolone and at least one of three injectable second-line drugs, such as Amikacin, Kanamycin, or Capreomycin [5]. So these clinical outcomes underline the need of new therapeutic entities with different mechanism of action to subside the situation.

Enoyl-ACP reductase (InhA) of *M. tuberculosis* , participate in the Fatty acid biosynthesis pathway (FAS II) by utilizing NADH to reduce the trans double bond of longer chain fatty acyl substrates for the purpose of synthesizing Mycolic acid ,an important factor for mycobacterium virulence [46] . InhA has been identified as the primary molecular target of INH, the first line drug for tuberculosis treatment. But clinical Isolates of *M. tuberculosis* resistant to INH are seen with increasing frequency (1 in 10^6) compared to other drugs [7]. Over other types of resistance, INH resistance was found to be in 10.3 %(new cases) and 27.3 %(treated cases) [8]. The biological activity of INH is reduced due to mutation in InhA and Kat G, a catalase/peroxidase enzyme responsible for generate bioactive form of INH [9-11].

Cinnamic acid and its derivatives are well established antimicrobial as well as anti-tubercular agents on and from several decades. Many clinical reports further demonstrated the efficacious role of cinnamates in treatment of tuberculosis [12-15]. These compounds also show synergistic activity with some first line anti-tubercular agent [16]. The precise mode of action of cinnamates as an anti-tubercular agent remains unidentified till date. Even though some study demonstrated that Cinnamic acid derivatives can be bound to cofactor binding site of InhA and the structural similarity of its enoyl-acyl backbone to the fatty acyl substrate of InhA, make them more reasonable topic for further research [17,18,]. Consequently the present study has done to describe the chemical features of existing bioactive cinnamic derivatives and to evaluate the key interaction with all feasible binding cavities of InhA (both Wild type and mutant protein) by means of computer aided molecular design (CAMD). Both ligand-based drug design (LBDD) and structure-based drug design (SBDD) methods were implemented for accomplish the total experiment and acquired computational information can reveal the crucial structural features of cinnamic acid derivatives as a potential class of anti-MDR tubercular agent.

2. Material and Method

2.1 General methodology

All pharmacophore and 3D QSAR models were generated by PHASE module of Maestro 9.1 software (Schrödinger LLC, New York) [19-21]. The protein structures were obtained from RCSB protein data bank (PDB) and docking studies were performed using JAGUAR and GLIDE module of MAESTRO 9.1 in extra precision (XP) mode [22].

2.2 Data set Preparation

For this study, a series of 44 compounds include thioester, amide, hydrazide, triazolophthalazine derivatives of 4-alkoxy and 4-hydroxy Cinnamic acid with some cyclopropyl derivatives, was collected from literature [25, 26]. The reported MIC (minimum inhibitory concentration) value was considered as biological activity property, estimated by *in vitro* assay of *M. tuberculosis* (H_{37}RV strain).These MIC values were subjected to corresponding logarithmic correction using the formula {act= -log (MIC)}[27].
The structures were drawn using Chemdraw Ultra 8.0 software [24].The 3D conversion and minimization steps were performed using OPLS 2005 Force field [27], with an implicit GB/SA solvent model, implemented in LigPrep Module. A maximum of 1,000 conformers were generated for each structure using pre-process minimization of 100 steps and post-process minimization of 50 steps. Each minimized conformer was filtered through a relative energy

window of 10 kcal mol^{-1} and a minimum atom deviation of 1.00 Å [19-21]. Then Single-point energy calculation, an *ab initio* quantum chemical method (B3LYP/6-31G**) was conducted in JAGUAR module using Density Functional Theory (DFT) for each molecule [28, 29]. An arbitrary adopting method was applied to divide the total data set into training set (70% of total molecule) and Test set (remain 30%) for validation purpose.

Table 1. Dataset of Cinnamic acid derivatives with corresponding pIC_{50} values.

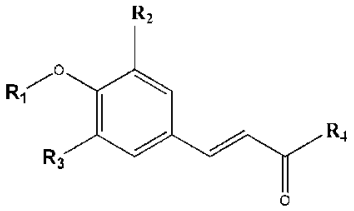

Compound	R1	R2	R3	R4	pIC_{50}
2a	Isopentenyl	H	H	N-acetylcysteamine	4.018
2b	Geranyl	H	H	N-acetylcysteamine	5.826
2c	Farnesyl	H	H	N-acetylcysteamine	5.894
2d	methyl	H	H	N-acetylcysteamine	3.647
2e	H	H	H	N-acetylcysteamine	3.624
2f	H	OCH_3	H	N-acetylcysteamine	3.373
2g	H	OCH_3	OCH_3	N-acetylcysteamine	3.415
3e	H	H	H	Thiophenyl	4.506
3f	H	OCH_3	H	Thiophenyl	4.554
4a	Isopentenyl	H	H	N-acetylethelenediamine	3.701
4b	Geranyl	H	H	N-acetylethelenediamine	6.585
5a	Isopentenyl	H	H	2-(1H-indol-3-yl)ethanamine	3.774
5b	Geranyl	H	H	2-(1H-indol-3-yl)ethanamine	4.141
5d	methyl	H	H	2-(1H-indol-3-yl)ethanamine	2.807
5f	H	OCH_3	H	2-(1H-indol-3-yl)ethanamine	4.624
6a	Isopentenyl	H	H	2-aminopyridine	4.285
6b	Geranyl	H	H	2-aminopyridine	5.576
6d	methyl	H	H	2-aminopyridine	3.606
6h	methyl	OCH_3	H	2-aminopyridine	3.357
10a	methyl	H	H	D-cycloserine	3.022
11a	methyl	H	H	INH*	6.523
11b	CF_3	H	H	INH*	5.959
11c	ethyl	H	H	INH*	5.886
11d	CF_3CH_2 -	H	H	INH*	5.658
11e	isopentenyl	H	H	INH*	5.638
11f	Geranyl	H	H	INH*	5.721
12a	methyl	H	H	Hydralazine	4.301
12b	CF_3-	H	H	Hydralazine	4.678
12c	ethyl	H	H	Hydralazine	4.921
12d	CF_3CH_2 -	H	H	Hydralazine	4.699
12e	isopentenyl	H	H	Hydralazine	4.678
12f	Geranyl	H	H	Hydralazine	4.143
13a	methyl	H	H	Triazolophthalazine	4.276

13b	CF_3-	H	H	Triazolophthalazine	3.154
13c	ethyl	H	H	Triazolophthalazine	4.409
13d	CF_3CH_2 -	H	H	Triazolophthalazine	3.77
13e	isopentenyl	H	H	Triazolophthalazine	5.854
13f	Geranyl	H	H	triazolophthalazine	4.721

Table 2. Cyclopropyl derivatives.

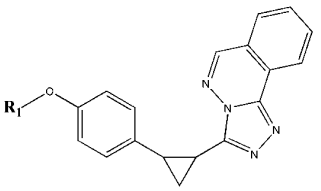

Compound	R_1	pIC_{50}
14a	methyl	3.40
14b	CF_3-	3.77
14c	ethyl	3.42
14d	CF_3CH_2	2.88
14e	isopentenyl	4.67
14f	Geranyl	4.55

** INH= Isoniazid, pIC_{50}= Observed biological activity.*

2.3 Generation of Pharmacophoric sites and common pharmacophore hypothesis

The structure of compound is defined by a set of points in 3D space, which communicate with different chemical features to facilitate non-covalent binding of the compound and its receptor. The six built-in pharmacophore features-hydrogen bond acceptor (A), hydrogen bond donor (D), hydrophobic group (H), negatively charged group (N), positively charged group (P) and aromatic ring (R) were used to create pharmacophoric sites. The pattern of pharmacophoric features are specified as SMARTS query [21, 30]. Common pharmacophore features were identified from a set of variants — a set of feature types that define a possible pharmacophore, using a tree-based partitioning algorithm with a maximum tree depth of five with the requirement that all actives must match. Scoring of pharmacophore hypothesis with respect to activity of ligand was conducted using default parameters for site, vector and volume terms. The activity threshold was set between 5.5 and 4.3 to define active and inactive ligands.

2.4 Building 3D QSAR model

An atom-based 3D QSAR model was generated by correlating the observed and estimated activity for training set of 31 molecules using Partial least square (PLS) regression analysis with grid spacing of 1.0 Å. The maximum number of PLS factor can be taken is N/5, where N is number of training set candidates. The best QSAR model was validated by predicting activity of the set of 13 test molecules.

2.5 Validation of QSAR model

An external validation method along with internal model validation techniques has been done simultaneously to justify the statistical significance of developed 3D-QSAR model. For external validation, R^2_{pred} parameter was considered which precisely reflects the degree of correlation between the observed and predicted property data [31]. The values of Q^2, $Q^2_{(F2)}$ and Pearson –R were also calculated as a parameter for external validation method [32].

2.6 Macromolecular preparation

The X-ray crystallographic structures of all protein molecules *viz.* wild type enoyl-acyl carrier protein reductase (ENR/InhA) with four more mutated variety (S94A, I21V, I47T,D148G) of this protein having clinical significance ,were retrieved from RCSB protein Data bank (http://www.rcsb.org/pdb, PDB ID: 2PR2, 2AQI, 2IE0, 4DQU,4DT1,1BVR,2NSD). The best proteins were selected by analyzing all entries with Ramachandran plot [33]

The protein structures co-crystallized with ligands or substrates were subjected for further refinement using PrepWizard module of Schrödinger software to add missing hydrogens, assign appropriate bond orders and formal charges, treating selenomethionines, di-sulfide bonds etc. Finally, energy minimization step was carried out with RMSD (root mean square deviation) value of 0.30 Å and using OPLS_2005 force field [34]

2.7 Molecular Docking

Receptor-Grid generation of prepared proteins, an important step in GLIDE docking protocol, is performed to pre-define the binding site for the ligands. The shape and the properties of the receptor are represented on a grid by several different sets of fields that provide progressively more accurate scoring of the ligand poses [35].

The docking studies were done for all prepared protein separately using GLIDE 5.5 module [35]. We engaged extra precision (XP) mode which uses Monte Carlo based simulated algorithm (MCSA) for minimization. The best docking poses with low Glide score and least binding energy was subjected for further investigation [36, 37].

3. RESULT AND DISCUSSION

3.1 Generation of pharmacophore model

Several five-featured common pharmacophore hypotheses with various combinations of sites were generated and the best hypotheses were selected on the basis of scoring function and selectivity. All training set compounds were aligned on best three selected hypotheses which consist of hydrogen bond acceptor (A), hydrophobic (H),hydrogen bond donor and ring feature (R) ,denoted as AADHR, AAAHR and AAADR. Each model was engaged for Partial Least Square (PLS) analysis with five PLS factor to avoid over-fitting of the result .The predictive ability of the model was re-evaluated by the test set compounds. As internal validation is not sufficient enough to define the predictive power of a QSAR model, we considered some external validation statistics (R^2_{Pred} and $Q^2_{(F2)}$) to choose best model (AAAHR) [38]. A summary of relevant statistical data of QSAR model is listed in Table-3. Graph of observed versus predicted biological activity of training and test set molecules are shown in Fig- 1.

Table 3. Summary of 3D QSAR results with external and internal validation.

ID	SD	R-squared	F	Q^2	Pearson-R	R^2_{Pred}	$Q^2_{(F2)}$
AADHR.11	0.0454	0.9983	2900.1	0.2601	0.5368	0.27	0.73
AAAHR.218	**0.1463**	**0.9848**	**324.6**	**0.8498**	**0.936**	**0.85**	**0.854**
AAADR.166	0.2856	0.9401	81.5	0.7369	0.9109	0.67	0.255

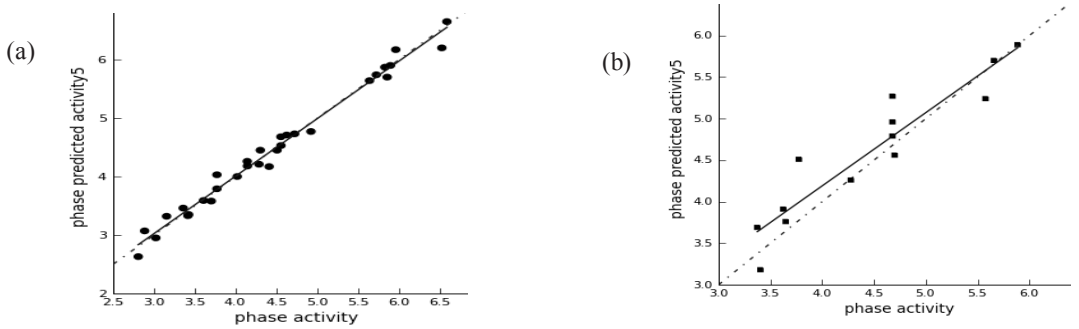

Fig. 1. Scatter plots for observed versus predicted biological activity of (a) training set and (b) test set compounds.

3.2 3D QSAR Analysis

PHASE 3D QSAR technique gives the advantage of visualizing feature-based counter cubes on favourable and unfavourable region in 3D space. The cubes obtained from statistically validated model AAAHR can illustrate the features important for interaction between ligands and target enzyme or receptor. In present representation, blue, green and cyan cubes indicate favourable region for H-bond acceptor, hydrophobic and electron withdrawing group respectively while red cubes express unfavourable region for biological activity. Comparative analysis of physico-chemical region is done with highest active (4b), lowest active (5d) and a reference molecule (11d) [Fig- 2]

Fig – 2(c, d) shows the green cubes generated for favourable hydrophobic region near CF_3CH_2- (R1) and INH (R4) group on both side of reference molecule (11d). This clearly indicates that substitution of hydrophobic group in these regions may increase biological activity. Therefore ,introduction of bulky Geranyl, Farnesyl groups in R1 position drastically increase the activity in highest active compounds like 4b,2b,2c,6b, and negatively regulates the activity on 5d,4d,2g,13b,10a molecules which lack off bulky substitutes. This discussion also gives an idea about the topology of receptor site.

Another crucial blue counter map or H-bond donor favourable region is found around Nitrogen atoms of hydrazide (-NH-NH-) group (R4 substitution) of reference molecule, which indicates the presence of secondary amino group can improve bioactivity [Fig. 2.e]. Therefore, Substitution of N-acetylethelenediamine, N-acetylcysteamine, pyridyl amides, INH in R4 position immensely increase activity of compounds (4b, 2b, 2c, 6b, 11b, 11c) and authenticates our observation. Red cubes indicates sterically unfavoured Donor property between two close –NH groups in 11d , which is overcome by N-acetylethelenediamine substitution in highest active compound(4b).

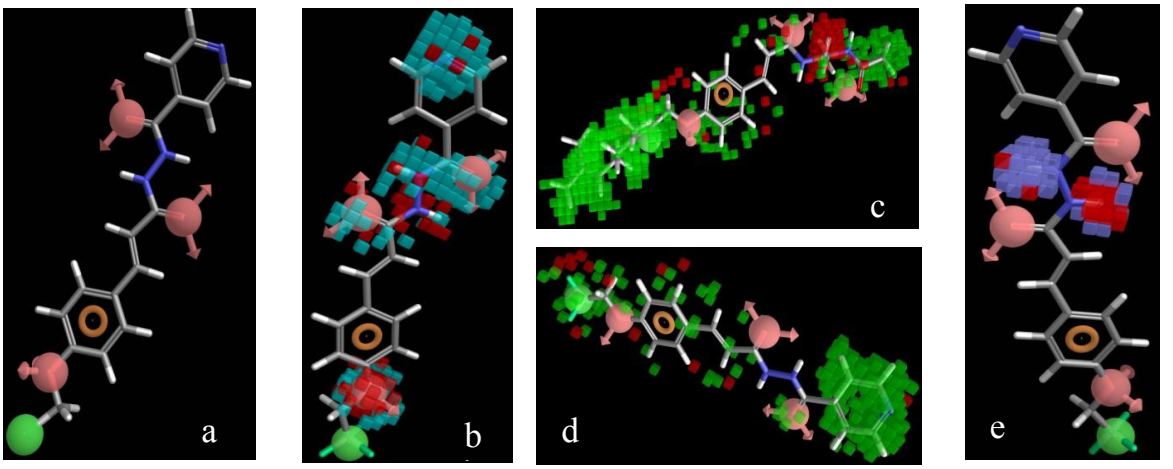

Fig. 2. (a) Alignment of best fit active molecule on AAAHR hypotheses. Red spheres with vector arrow represent the acceptor (A) properties, green sphere for hydrophobic (H) and brown ring denotes aromatic ring feature(R).(b-e) cyan, green and blue cubes are favourable regions respectively for electron-withdrawing, hydrophobic and H-bond donor features and red cubes denotes unfavourable area for respective features.

3.3 Docking results

The docking simulation was performed using GLIDE (Grid based ligand docking with energetics) program with energy calculated ligands. The set of ligands were included with Isoniazid and Isoniazid-NAD adduct for comparative binding mode study.

Pathway analysis and structural studies on ligand bound protein complex have revealed three putative binding clefts of InhA, (i) cofactor NADH binding pocket, (ii) fatty acyl substrate binding site and (iii) the pocket into which the isonicotinoyl group of INH-NAD sticks out [39-41]. The molecules were docked into each site also with mutant varieties and each docking simulation model was assayed separately [Fig. 5].

3.4 Binding mode analysis

3.4.1 Docking with co-factor binding site of wild-type and mutatated protein

Co –factor(NADH) binding pocket is also competitively occupied by INH-NAD adduct, a slow and tight binder of InhA [34] .Here we conducted molecular docking with Wt InhA(2PR2) and S94A, I21V, I47T,D148G (INH resistant) mutated InhA in complex with NADH or INH-NAD. Docking pose of both aforesaid ligands reveal that H-bond interaction with residues like Ser 20,Gly14, Gly 96, Lys 165,Ile 21, Val65 ,Asp 64, Ile 194 ,Ser 94, Ala 198 ,Thr 17 ,Thr 196 and a profound hydrophobic pocket (surrounded by Phe 41, Ile 122, Leu 63, Val 65 , Ile 95, Phe 97, Lys 118, Ile 16) provides for binding. Molecules with good binding affinity (5b, 5a, 3f, and 11d) have nicely engaged the hydrophobic region and no H-bond interaction with glycin-rich loop make these more feasible for INH-resistant strains [42-44]. Oxygen atom of enoyl-acyl back bone of compounds made important H-bond, where absent of this property in cyclopropyl derivatives (14a-14f) decrease its bio-activity.

3.4.2 Docking into the binding site of direct InhA inhibitor

The isonicotinoyl moieties of the INH-NAD and Ethionamide (ETH)-NAD adduct were inserted in a hydrophobic pocket formed with a flexible side-chain of residue Phe 149. The cavity was situated below the fatty acyl substrate-binding site and, lined prominently by hydrophobic residues of Tyr 158, Phe 149, Met199, Trp 222, Leu 218, Met155, Met161, Gly192, and Pro193 [42] [Fig. 4.b]. Study showed that bulky aliphatic substitution, most preferably isopentenyl group in R1 position, perfectly occupied the cavity and enhanced the binding affinity drastically (e.g. compound 6a, 4a.2a, 12e, 11e, 11f). Along with that, two crucial H-bonds between the O atom of enoyl chain of cinnamic acid scaffold with Tyr 158 and co-factor NADH, co-crystallized with enzyme, perfectly supports result of 3D QSAR analysis.

3.4.3 Interaction with substrate binding region

InhA, a member of FAS II pathway prefers longer chain fatty acyl substrates which is engulfed by substrate binding hydrophobic loop (residue 196-219) [45] . Present study reveals that hydrophobic residues like Tyr 158, Phe 149, Pro 193, Ile 215, Leu 218, Ile 202, Ala 198, Ala 201 and Leu 207 acquire important role in interaction. The benzene ring of cinnamates with aliphatic chain substitution played decisive role in hydrophobic entrapment. Compound 5f, 13f, 3f, 4b, 5b, 2b etc were identified on the basis of XP docking score, docking energy and 0hydrophobic enclosure reward

All structure-based docking simulation models show good complementarities with 3D QSAR model. Direct inhibitor model is observed as most definitive to QSAR result.

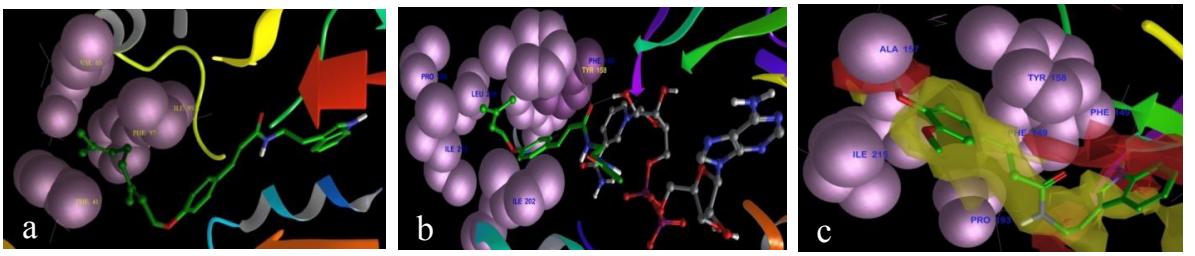

Fig.4. Hydrophobic part in CPK representation of (a) co-factor binding site, (b) direct inhibitor binding cavity and (c) substrate binding site which are docked with ligands having highest binding affinity.

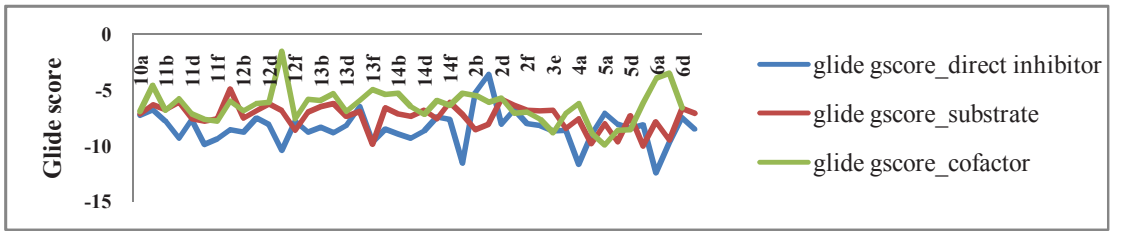

Fig. 5. Docking score distribution chart for all three types of docking simulation.

4. CONCLUTION

We have investigated the significances of various structural features of cinnamic acid derivatives as a potential anti-tubercular agent using the hybrid *in silico* docking and pharmacophore mapping approaches. Our predicted activity data for the cinnamic acid derivatives displays excellent correlations with the experimental activity, confirming the accuracies of our simulations. Our docking results demonstrate that the top orders against the InhA enzymes are dominated by bulky hydrophobic groups, H-bond acceptors and aromatic ring property, and these features also show excellent conformity with ligand-based pharmacophore model. Further exploration on these structural guidelines and development of new computational intelligence screening tools using this combined structure-guided model, may be helpful to assay chemical spaces for design of the novel inhibitors against MDR strains.

Acknowledgements

We acknowledge Schrodinger LLC Bangalore, India for their eminence support and assistance.

Reference

[1] World Health Organization Ninth Annual Report on Tuberculosis.2004. Global tuberculosis control:surveillance, planning, financing. Global Tuberculosis Report 2012, WHO. (2012)

[2] Cole, ST., and Alzari PM. Towards new tuberculosis drugs. Biochemical SocietyTransactions, (2007), 35, Part 5, 1321-1324. ISSN: 0300-5127.

[3] Dye C. Global epidemiology of tuberculosis. Lancet, (2006), 367, No.9514, 938-40. ISSN: 0140-6736.

[4] Nunn, P., Williams, B., Floyd, K., Dye, C., Elzinga, G. & Raviglione, M. Tuberculosis Control in the Era of HIV, Nature Reviews Immunology, (2005), 5, No.10, 819-826

[5] Multidrug-resistant tuberculosis (MDR-TB), Region, W H O,2013

[6] Quémard A, Sacchettini JC, Dessen A, Vilcheze C, Bittman R, Jacobs WR, Jr, Blanchard JS. Enzymatic characterization of the target for isoniazid in Mycobacterium tuberculosis.Biochemistry. (1995), 34(26), 8235–8241.

[7] Nachega JB, Chaisson RE, Tuberculosis Drug Resistance: A Global Threat. Clin. Infect. Dis, (2003), 36, [Suppl 1], 24-30,

[8] World Health Organization: International Union Against Tuberculosis and Lung Disease. Global Project on Anti-Tuberculosis Drug Resistance Surveillance. 2002-2007. Fourth Global Report (2008).

[9] Quémard, A., A. Dessen, M. Sugantino, W. R. Jacobs Jr., J. C. Sacchettini, and J. S. Blanchard.. Binding of catalase-peroxidase-activated isoniazid to wild-type and mutant *Mycobacterium tuberculosis* enoyl-ACP reductases. J. Am. Chem. Soc.(1996), 118, 1561–1562

[10] Johnsson, K., D. S. King, and P. G. Schultz. Studies on the mechanism of action of isoniazid and ethionamide in the chemotherapy of tuberculosis. J. Am. Chem. Soc. (1995), 117, 5009–5010.

[11] Basso, L. A., R. Zheng, and J. S. Blanchard.. Kinetics of inactivation of WILD-TYPE and C243S mutant of *Mycobacterium tuberculosis*: enoyl reductase by activated isoniazid. J. Am. Chem. Soc. (1996), 118, 11301–11302.

[12] Warbasse, J.P. Cinnamic Acid in the Treatment of Tuberculosis, Annals of Surgery, (1894), 19, 102-117.

13. Jacobson, M.J. Ethylcinnamate in Experimental Tuberculosis, Bulletins et Mémoires de la Société Médicale des Hôpitaux de Paris, (1919), 35, 322-325.

[14] Corper, H.J., Gauss, H. & Gekler, W.A. Studies on the Inhibitory Action of Sodium Cinnamate in Tuberculosis. Colorado American Review of Tuberculosis, (1920), 4, 464- 473.

[15] Gainsborough, H. A Note on the Use of Benzyl Cinnamic Ester in Tuberculosis, The method of Jacobsen. Lancet, (1928), Vol.211, No.5462, 908-909.

[16] Rastogi, N.; Goh, K. S.; Horgen, L.; Barrow, W. W. FEMS, Synergistic activities of antituberculous drugs with cerulenin and trans-cinnamic acid against *Mycobacterium tuberculosis*, Immunol. Med. Microbiol.(1998), 21, 149.

[17] Lu.H,Tonge . P. Inhibitors of FabI, an enzyme drug target in the bacterial fatty acid biosynthesis pathway, J . Acc. Chem . Res. 2008, 41, 11.

[18] Carvalho. S. A.;da Silva. E. F.; De souza M.V.N.; Lourenco M. C. S.;Vicente. F.R. Synthesis and antimycobacterial evaluation of new trans-cinnamic acid hydrazide derivatives, Bioorg. Med . chem. Let. (2008), 18 ,538.

[19] Phase 1.0 (2005) User manual. Schrodinger, New York.

[20] Dixon, S. L.; Smondyrev, A. M.; Knoll, E. H.; Rao, S. N.; Shaw, D. E.; Friesner, R. A., "PHASE: A New Engine for Pharmacophore Perception, 3D QSAR Model Development, and 3D Database Screening. 1. Methodology and Preliminary Results," J. Comput. Aided Mol.

Des., (2006), 20, 647-671.

[21] Dixon, S. L.; Smondyrev, A. M.; Rao, S. N. "PHASE: A Novel Approach to Pharmacophore Modeling and 3D Database Searching," Chem. Biol. Drug Des., (2006), *67*, 370-372.

[22] R.A. Friesner, R.B. Murphy, M.P. Repasky, L.L. Frye, J.R. Greenwood, T.A. Halgren, P.C. Sanschagrin, D.T. Mainz, Extra precision Glide: docking and scoring incor-porating a model of hydrophobic enclosure for protein–ligand complexes, J. Med. Chem. (2006), 49, 6177–6196.

[23] Bhattacharjee. A. , Mylliemngap B.J. and Velmurugan. D. , '3D-QSAR Studies on Fluroquinolones Derivatives as Inhibitors for Tuberculosis', Bioinformation, 8 (2012).

[24] Mills, N. "ChemDraw Ultra 10.0". *J. Am. Chem. Soc.* (2006), 128 (41): 13649–13650.

[25] Yoya, G. K., Bedos-Belval, F., Constant, P., Duran, H., Daffé, M. & Baltas. M. Synthesis and Evaluation of a Novel Series of Pseudo-Cinnamic Derivatives as Antituberculosis Agents, Bioorganic & Medicinal Chemistry Letters, (2009), 19, No.2, 341-343.

[26] De, P., Yoya, G.K., Constant, P., Bedos-Belval, F., Duran, H., Saffon, N., Daffé, M. & Baltas M. Design, Synthesis and Biological Evaluation of New Cinnamic Derivatives as Antituberculosis Agents, Journal of Medicinal Chemistry, (2011), 54, No.5,1449 -1461.

[27] Halgren TA. MMFF VI: MMFF94s option for energy minimization studies. J Comp Chem,(1999), 20, 720–729.

[28] *Computational Chemistry*, David Young, Wiley-Interscience, 2001. Appendix A. A.2.5 pg 337, Jaguar.

[29] Vondrášek et.al. "Unexpectedly strong energy stabilization inside the hydrophobic core of small protein rubredoxin mediated by aromatic residues: correlated ab initio quantum chemical calculations". *Journal of the American Chemical Society,* (2005), **127** (8): 2615–2619.

[30] SMARTS – Language for Describing Molecular Patterns, Daylight Chemical Information Systems,Inc., AlisoViejo,CA.

[31] Sabrina G. R. Mota; Tânia F. Barros; Marcelo S. Castilho,"2D QSAR studies on a series of bifonazole derivatives with antifungal activity" J. Braz. Chem. Soc. (2009), 20, no.3.

[32] Consonni V, Ballabio D, Todeschini R, Comments on the definition of the Q2 parameter for QSAR validation**,**J Chem Inf Model. (2009), 49(7), 1669-78.

[33] Ramachandran, G.N.; Ramakrishnan, C.; Sasisekharan, V. "Stereochemistry of polypeptide chain configurations". *Journal of Molecular Biology*. (1963), **7**, 95.

[34] Schrödinger Suite 2009 Protein Preparation Wizard, Schrödinger, LLC, New York, NY, (2009)

[35] Glide, Version 5.5, (2009) Schrodinger, LLC, New York, NY.

[36] Halgren, T. A., Murphy, R. B., Friesner, R. A., Beard, H. S., Frye, L. L. Pollard, W. T., Banks, J. L. Glide: A new approach for rapid, accurate docking and scoring. 2. Enrichment factors in database screening. J Med Chem. (2004), 47, 1750–1759.

[37] Hamilton Miller, J. M. T. Antimicrobial Properties of Tea (Camellia sinensis L.) Antimicrob. Agents and Chemother. (1995), 39, 2375–2377.

[38] Tropsha A, Gramatica P, Gombar VJ . "The Importance of Being Earnest: Validation is the Absolute Essential for Successful Application and Interpretation of QSPR Models". *QSAR &Comb. Sci.* (2003), 22, 69–77.

[39] Delaine T, et al. Development of isoniazid-NAD truncated adducts embedding a lipophilic fragment as potential bi-substrate InhA inhibitors and antimycobacterial agents. Eur. J. Med. Chem. (2010), 45, 4554–4561.

[40] T. Delaine, V. Bernardes-Génisson, A. Quémard, P. Constant, F. Cosledan, B. Meunier and J. Bernadou, Preliminary Investigations of the Effect of Lipophilic Analogues of the Active Metabolite of Isoniazid Toward Bacterial and Plasmodial Strains, *Chem. Biol. Drug Des.* (2012), 79, 1001–1006.

[41] Freundlich JS, Wang F, Vilcheze C , Gulten G, Lang ley R , Schiehser GA, Jacobu s DP, Jacobs WR, Jr, Sacchet tini JC Triclosan derivatives: towards potent inhibitors of drug-sensitive and d rug-resistant *Mycobacterium tuberculosis*. ChemMedChem. (2009), 4, 241-248.

[42] Rescigno, M., and R. N. Perham. Structure of the NADPH-binding motif of glutathione reductase:efficiency determined by evolution. Biochemistry. (1994), 33, 5721–5727.

[43] Nishiya, Y., and T. Imanaka. Analysis of interaction between the Arthrobacter sarcosine oxidase and the coenzyme flavin adenine dinucleotide by site-directed mutagenesis. Appl. Environ. Microbiol. (1996), 62, 2405–2410.

[44] Eschenbrenner, M., L. J. Chlumsky, P. Khanna, F. Strasser, and M. S. Jorns. Organization of the multiple coenzyme and subunits and role of the covalent flavin link in the complex heterotetrameric sarcosine oxidase. Biochemistry. (2001), 40, 5352–5367.

[45] Denise A Rozwarski and others, 'ENZYMOLOGY : Crystal Structure of the Mycobacterium Tuberculosis Enoyl-ACP Reductase , InhA , in Complex with NAD+ and a C16 Fatty Acyl Substrate *'.The Journal of Biological Chemistry, (1999), 274, 15582-15589.

[46] Zhang Y, Garbe T, Young D. Transformation with katG restores isoniazid-sensitivity in Mycobacterium tuberculosis isolates resistant to a range of drug concentrations. Mol Microbiol.(1993), 3, 521–524